0031-3998/11/6903-0249
PEDIATRIC RESEARCH

Vol. 69, No. 3, 2011
Printed in U.S.A.

Development of Corpus Callosum in Preterm Infants Is Affected by the Prematurity: *In Vivo* Assessment of Diffusion Tensor Imaging at Term-Equivalent Age

TATSUJI HASEGAWA, KEI YAMADA, MASAFUMI MORIMOTO, SHIGEMI MORIOKA, TAKENORI TOZAWA, KENICHI ISODA, AKI MURAKAMI, TOMOHIRO CHIYONOBU, SACHIKO TOKUDA, AKIRA NISHIMURA, TSUNEHIKO NISHIMURA, AND HAJIME HOSOI

Department of Pediatrics [T.H., M.M., S.M., T.T., K.I., A.M., T.C., S.T., A.N., H.H.], Department of Radiology [K.Y., T.N.], Graduate School of Medical Science, Kyoto Prefectural University of Medicine, Kyoto 602-8566, Japan

ABSTRACT: Callosal injury in preterm infants is a key factor affecting neurodevelopmental outcome. We investigated the characteristics of corpus callosum (CC) in preterm infants without apparent white matter lesions. We studied 58 preterm infants divided into three groups of 23–25, 26–29, and 30–33 wk GA. Diffusion tensor imaging (DTI) was obtained at term-equivalent age. The CC was parcellated into the genu, body, isthmus, and splenium. We measured fractional anisotropy (FA) and apparent diffusion coefficient (ADC) of each CC subdivision using tractography and manual region of interest analysis. The cross-sectional areas were also measured. At the isthmus and splenium in the 23–25 GA group, the FA was significantly lower and the size was also significantly reduced. Furthermore, the FA and cross-sectional areas in the posterior CC decreased linearly with decreasing GA. There were no differences in FA and cross-sectional areas in other CC subdivisions, and no differences in ADC in any CC subdivisions, among the GA groups. We demonstrated that preterm infants without apparent white matter lesions affect development of the posterior CC depending on the degree of prematurity. **(*Pediatr Res* 69: 249–254, 2011)**

Mortality rates of preterm infants have decreased in recent years primarily because of the development of neonatal intensive care (1,2). However, there are persistently high rates of neurodevelopmental impairments among preterm infants who survive (1,2), including major motor deficits (*e.g.* CP), cognitive deficits, neurosensory impairments, attention deficit/hyperactivity disorder, and learning disabilities (3,4). The most important brain abnormalities of prematurity are cerebral white matter (WM) injury and periventricular leukomalacia (PVL), with the latter being the main cause of motor deficits (5).

The corpus callosum (CC) is the main WM connection between the two hemispheres and plays important roles in cognitive (*e.g.* speech and language) and behavioral functions (6–8). Magnetic resonance (MR) studies at childhood to adolescence have indicated that such functional impairments of preterm born individuals are associated with smaller size of the CC (6,9–12). Thus, the degree of callosal injury in preterm infants is considered an important factor that strongly affects neurodevelopmental outcome.

Received June18, 2010; accepted October 12, 2010.
Correspondence: Masafumi Morimoto, M.D., Ph.D., 465 Kajii-cho, Kawaramachi-Hirokoji, Kamigyo-ku, Kyoto 602-8566, Japan; e-mail: morimoto@koto.kpu-m.ac.jp

Recent advances in diffusion tensor imaging (DTI) and DTI-based tractography have enabled new approaches to investigate the structure of WM tracts *in vivo* (13). By use of diffusion parameters such as fractional anisotropy (FA) and apparent diffusion coefficient (ADC), it is possible to quantitatively assess WM changes that are not apparent on conventional MRI. In general, FA increases and ADC decreases with age, which is believed to reflect WM maturation such as fiber coherence, axonal density, and myelination (14–19). By contrast, WM injury can result in lower FA and higher ADC. This approach is useful in assessing microstructural WM injury and has been used in preterm infants at term-equivalent age (20–23). If the characteristics of callosal injury in preterm infants can be reliably assessed using DTI at term-equivalent age, this may allow prediction of later neurodevelopmental outcome.

The aim of our study was to investigate whether callosal injury in preterm infants exhibits a characteristic distribution and a relationship with prematurity. We parcellated the CC into four parts (genu, body, isthmus, and splenium) and assessed each part using both two-dimensional region of interest (ROI) analysis and tractography. Furthermore, because the relationship between the degree of callosal injury and prematurity is unknown, we assessed the correlation between the measured parameters and GA at birth.

METHODS

This study was approved by the Kyoto Prefectural University of Medicine Research Ethics Committee, and written informed consent was obtained from the parents of each patient.

Patients. MRI was performed on 146 infants who were admitted to the NICU at University Hospital, Kyoto Prefectural University of Medicine, between July 2005 and July 2008 for clinical diagnosis purposes before discharge. Among these 146 infants, 24 were excluded as they had no DTI or DTI was degraded because of motion artifact. Of the remaining 122 infants, we first performed quantitative DTI assessment with blinding to the conventional MR findings and clinical details. Inclusion criteria were as follows: 1) <34 wk GA at birth, 2) no evidence of brain abnormalities such as PVL and intraventricular hemorrhage grade III-IV on cranial sonography or conventional MR, and 3) scanning MR at term-equivalent age (ranging from 37 to 43 wk corrected GA). Sixty-four infants were excluded from the study, and the

Abbreviations: ADC, apparent diffusion coefficient; **CC,** corpus callosum; **DTI,** diffusion tensor imaging; **FA,** fractional anisotropy; **MR,** magnetic resonance; **OL,** oligodendrocyte; **PVL,** periventricular leukomalacia; **ROI,** region of interest; **WM,** white matter

Table 1. *Characteristics of preterm infants in each GA group*

	Group A	Group B	Group C	*p*
n	10	23	25	
Male/female	6/4	13/10	12/13	0.90
At birth				
GA (wk)	24.72 (23.00–25.86)	28.12 (26.14–29.71)	32.10 (30.14–33.71)	
Birth weight (g)	718 (554–932)	973 (556–1405)	1425 (706–2012)	
Head circumference (cm)	21.8 (19.5–22.8)	25.1 (22.0–28.0)	28.4 (24.0–31.7)	
At MR scanning				
Corrected GA (wk)	40.43 (38.00–43.71)	40.10 (37.43–43.71)	39.22 (37.86–43.71)	0.16
Body weight (g)	2158 (1974–2382)*	2291 (2006–2674)	2328 (1768–2742)	0.03
Head circumference (cm)	32.6 (30.6–35.0)	33.4 (32.0–35.3)	33.3 (31.0–34.8)	0.12

Groups A, B, and C consist of infants born at 23–25, 26–29, and 30–33 wk GA, respectively. Measurement values indicate mean (range).
* $p < 0.05$ *vs* group C for post hoc test.

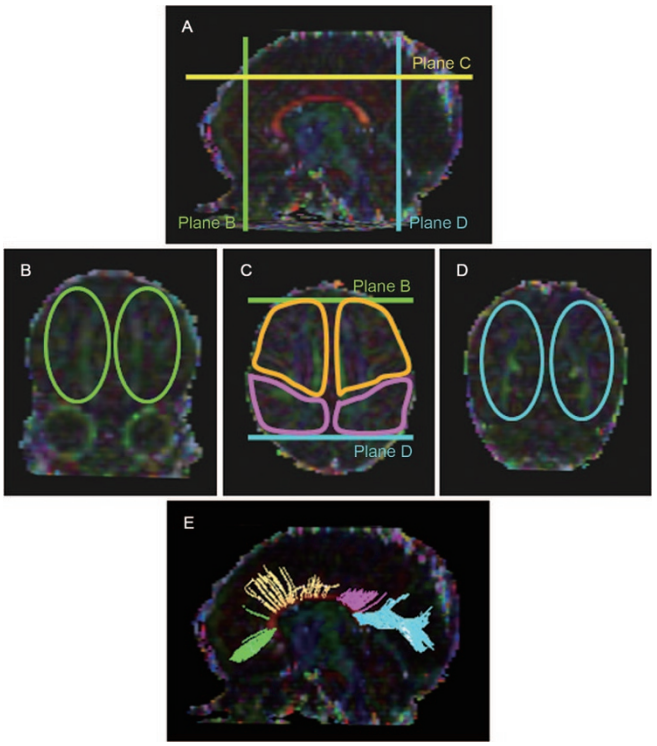

Figure 1. Locations of ROIs depicting each callosal tract using tractography. All images are shown on an FA color map. (*A*) Midsagittal slice image. The three lines show the planes for placement of ROIs for each callosal tract. (*B*) Coronal slice at the one third of the distance between the anterior edge of the genu and the most anterior tip of the hemisphere. (*C*) Axial slice at the corona radiata level. (*D*) Coronal slice at the one third of the distance between the posterior edge of the splenium and the most posterior tip of the hemisphere. *Green*, *orange*, *purple*, and *blue circles* are regions with ROIs placed to identify tracts through the genu, body, isthmus, and splenium, respectively. (*E*) Image shows each callosal tract. *Green*, *orange*, *purple*, and *blue fibers* show tracts passing through the genu, body, isthmus, and splenium, respectively.

remaining 58 preterm infants (31 males and 27 females) met our inclusion criteria.

The 58 infants were divided into three birth GA groups: group A, 23–25 wk GA (six males and four females); group B, 26–29 wk GA (13 males and 10 females); and group C, 30–33 wk GA (12 males and 13 females). Characteristics of the preterm infants in each group are shown in Table 1. There were no significant differences in sex, corrected GA, or head circumference at MR among the GA groups. However, body weight at MR was significantly different among the three GA groups ($p = 0.03$), and group A was significantly lower than group C on post hoc analysis ($p < 0.05$).

Imaging. MR images were obtained using a 1.5-T whole-body scanner (Gyroscan Intera; Philips Medical Systems, Best, The Netherlands) with a gradient strength of 30 mT/m. All transaxial slices were obtained using a plane parallel to the anterior commissure-posterior commissure (AC-PC) line. A single-shot echo-planar imaging (EPI) technique was used for DTI with motion-probing gradient in 15 orientations using the following parameters: TR 6000 ms, TE 88 ms, matrix 128 × 128, field of view 200 × 200 or 230 × 230, slice thickness 2.5 or 3.0 mm (voxel size = 1.56 × 1.56 × 2.5, 1.56 × 1.56 × 3.0, or 1.8 × 1.8 × 3.0 mm^3), and *b*-value = 0 and 1000 s/mm^2. Field of view and slice thickness were determined by the size of each brain. The voxel sizes applied in each GA group were as follows: group A, 1.56 × 1.56 × 2.5 mm^3 in five (50%), 1.56 × 1.56 × 3.0 mm^3 in one (10%), and 1.8 × 1.8 × 3.0 mm^3 in four (40%) infants; group B, 1.56 × 1.56 × 2.5 mm^3 in 13 (57%), 1.56 × 1.56 × 3.0 mm^3 in seven (30%), and 1.8 × 1.8 × 3.0 mm^3 in three (13%) infants; and group C, 1.56 × 1.56 × 2.5 mm^3 in 18 (72%), 1.56 × 1.56 × 3.0 mm^3 in two (8%), and 1.8 × 1.8 × 3.0 mm^3 in five (20%) infants. The χ^2 test showed no significant difference in voxel sizes among the GA groups ($p = 0.13$). The scanning time for DTI data were 264 s.

The infants were sedated for imaging with oral triclofos sodium (70–80 mg/kg) at 30–60 min before MR scanning. Ear protection was used for each infant throughout the MR examination. Infants were observed by pediatricians before, during, and after the examination.

Quantitative tractography. DTI data were transferred to an offline workstation for analysis. PRIDE software (Philips Medical Systems, Amsterdam, The Netherlands) was used for image analysis. ROI placement was determined based on identifiable anatomical landmarks by the FA color map or $b = 0$ image. DTI were measured by a single operator (T.H.) for consistency in the placement of ROIs. We used an FA threshold of 0.15 as the stop criteria as the FA of gray matter is typically in the range 0.1–0.2, and the immature WM has a lower FA compared with during childhood and adulthood where the FA threshold is generally 0.2 (13).

Callosal tracts were parcellated into four tracts that passed through the genu, body, isthmus, and splenium. To depict each callosal tract, we used the modified methods previously described (24,25). Two ROIs were manually placed on a specific cortical area in both hemispheres (Fig. 1) and were defined as follows. The tract through the genu was identified by placing ROIs on the prefrontal area at one third of the distance between the genu and the anterior tip of the hemisphere on a coronal slice (Fig. 1*B*). The ROIs to depict tracts projecting from the body and isthmus were set on the premotor and primary motor area and the ventral part of the parietal lobe, respectively, on an axial slice through the corona radiata (Fig. 1*C*). The tract through the splenium was identified by placing ROIs at one third of the distance between the splenium and the posterior tip of the hemisphere on a coronal slice (Fig. 1*D*). These ROIs included the dorsal part of the parietal lobe and the whole occipital lobe. Thus, four callosal tracts were depicted (Fig. 1*E*).

Parcellation of the CC and assessment with ROI analysis and area measurement. In addition to tractography, we also assessed regional changes in CC subdivisions using ROI analysis and area measurement. The CC was parcellated into four subdivisions using previously described methods (Fig. 2*A*) (26); the four subdivisions were the genu including rostrum, body composed of rostral body, anterior midbody, and posterior midbody, isthmus, and splenium (Fig. 2*B*). According to previous tractography studies on connections of CC subdivisions with cortical areas (24,27,28), our method for CC parcellation indicated that each CC subdivision largely corresponded to the region through each callosal tract. On the basis of this parcellation, we manually delineated and placed the ROI on the CC at the midsagittal slice using a color vector map, on which the CC was encoded red (representing orientation of right-left to direction). The procedure was as follows. First, we placed the ROI on the whole CC and counted the number of voxels and anteroposterior length in this ROI. Second, according to CC parcellation

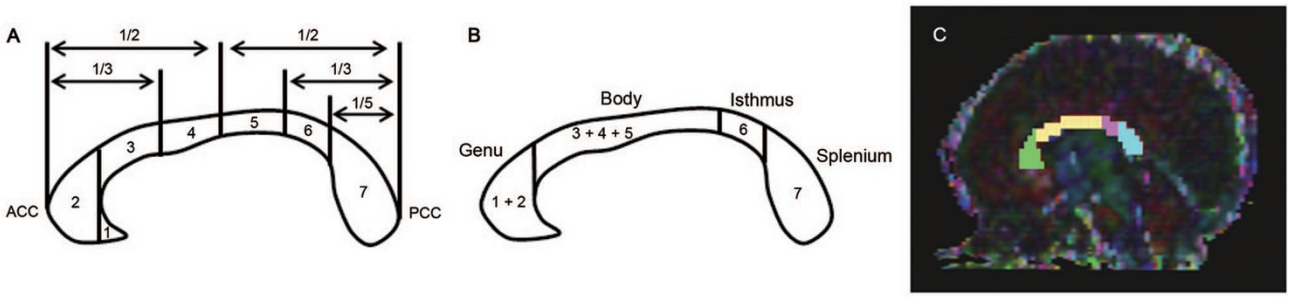

Figure 2. Scheme for parcellation of the CC and ROI placement for ROI analysis. (*A*) Witelson's classification for parcellation of the CC. The seven subdivisions were (1) rostrum, (2) genu, (3) rostral body, (4) anterior midbody, (5) posterior midbody, (6) isthmus, and (7) splenium. (*B*) Parcellation of the CC in our study. Our four subdivisions were the genu including (1) and (2), body composed of (3), (4), and (5), isthmus (6), and splenium (7). Image (*C*) shows four ROIs placed on each CC subdivision at midsagittal image, according to our method for CC parcellation. *Green*, *orange*, *purple*, and *blue* ROIs were placed on the genu, body, isthmus, and splenium, respectively.

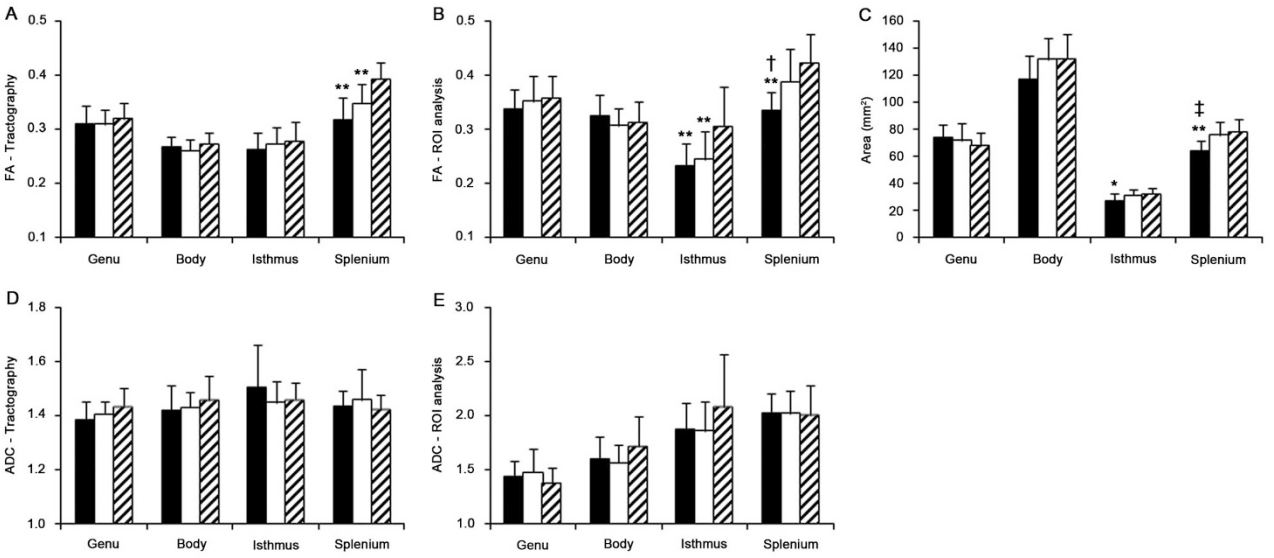

Figure 3. Comparisons of FA and ADC measured by DTI and size of each CC subdivision among the three GA groups. Bar graph showing FA (*A*) and ADC (*D*) measured by tractography, FA (*B*) and ADC (*E*) measured by manual ROI analysis, and size (*C*). *Black*, *white*, and *hatched bars* show measurements of groups A, B, and C, respectively. Units for ADC are 10^{-3} mm^2/s. There were significant differences in FA measured by tractography of the splenium ($p < 0.001$), FA measured by manual ROI analysis of the isthmus ($p = 0.003$) and splenium ($p < 0.001$), and the size of the isthmus ($p = 0.022$) and splenium ($p < 0.001$) among three GA groups. †$p < 0.05$, ‡$p < 0.01$ *vs* group B; *$p < 0.05$, **$p < 0.01$ *vs* group C for post hoc test.

applied in this study, the number of voxels in each CC subdivision was calculated and converted to millimeters squared using the voxel size information. Finally, we placed the ROI for the FA/ADC measurements on each CC subdivision, similar to the number of voxels and the length of the ROI calculated for area measurements (Fig. 2*C*). To avoid variance, we repeated the measurements three times and the averaged values of three measurements were used for statistical analysis.

Statistical analysis. Diffusion parameters and cross-sectional area data were examined for multiple comparisons among the three GA groups using the Kruskal Wallis *H* test, the nonparametric equivalent of the parametric one-way ANOVA. When the Kruskal Wallis *H* test showed a significant difference, we used Scheffe's *F* test for multiple comparisons as a post hoc analysis. The χ^2 test was used for analysis of the effects of gender among the three GA groups. Correlations between diffusion parameters or CC subdivision area and GA at birth were examined by Spearman's correlation, and $p < 0.05$ was considered statistically significant.

RESULTS

Quantitative tractography measurements. Tractography measurements of FA and ADC in each callosal tract for the three GA groups are shown in Figure 3*A* and *D*. The FA of the tract through the splenium was markedly different among the GA groups ($p < 0.001$), with a significantly lower FA in group A and group B compared with group C on post hoc test ($p < 0.01$). The FA values in the other callosal tracts were not significantly different among the GA groups. There were no differences in ADC values in any callosal tracts among the GA groups.

Manual ROI analysis measurements. ROI measurement results of each CC subdivision are shown in Figure 3*B* and *E*. The FA of the isthmus and splenium were different among the three GA groups (isthmus, $p = 0.003$; splenium, $p < 0.001$). In the isthmus, group A and group B had a significantly lower FA than group C on post hoc test ($p < 0.01$). In the splenium, group A had a significantly lower FA than group B and group C ($p < 0.05$ and $p < 0.01$, respectively). There were no differences in FA values in the genu or the body among the GA groups. There were no differences in ADC values in any callosal tracts among the GA groups.

Cross-sectional area. Area measurements of the CC subdivisions are shown in Figure 3*C*. There were significant differences in the sizes of the isthmus and the splenium among the three GA groups (isthmus, $p = 0.022$; splenium, $p < 0.001$). The isthmus of group A was significantly smaller than group C ($p < 0.05$), and the splenium of group A was significantly smaller than group B and group C ($p < 0.01$) on post hoc tests. Although the sizes of the whole CC, genu, and body were not different among the GA groups, the whole CC and the body area of group A had a tendency to be smaller than the other groups (whole CC, $p = 0.053$; body, $p = 0.051$).

Analysis of the posterior CC. As our data suggested that the posterior CC, especially the splenium, was markedly different in the younger GA groups, we hypothesized that posterior CC damage was dependent on the degree of prematurity. Thus, we examined whether GA at birth was associated with FA and size of the isthmus and splenium, respectively. The relationship between GA at birth and FA of the tract through the posterior CC depicted by tractography is shown in Figure 4*A* and *D*. The FA of the tract through the splenium was strongly correlated with GA at birth ($p < 0.001$, $r = 0.70$). There was no correlation between FA of the tract through the isthmus and GA at birth ($p = 0.16$, $r = 0.18$). For manual ROI analysis measurements, FA values of both the isthmus (Fig. 4*B*) and the splenium (Fig. 4*E*) were correlated with GA at birth (isthmus, $p < 0.001$, $r = 0.51$; splenium, $p < 0.001$, $r = 0.59$). The manually measured areas of both the isthmus (Fig. 4*C*) and the splenium (Fig. 4*F*) in the posterior CC were significantly correlated with GA at birth (isthmus, $p = 0.013$, $r = 0.33$; splenium, $p = 0.002$, $r = 0.42$).

DISCUSSION

To evaluate the potential callosal injury caused by prematurity, we studied infants born preterm without apparent WM lesions at term-equivalent age by conventional MRI. We investigated the relationship between measured CC parameters and GA at birth. Our primary finding was that FA of the posterior CC was lower in subjects with younger GA at birth and that FA decreased linearly with GA at birth. More specially, the FA of the tract through the splenium as measured by tractography and the FA of the isthmus/splenium as measured by ROI analysis were both significantly decreased in younger GA groups. Callosal injury is a well-established accompanying finding of PVL (29,30). However, as our subjects had no apparent WM lesions on conventional MR, these data suggest that development of the posterior CC may be affected because of the prematurity of the infants.

The FA decline observed in the CC of younger GA infants was most marked in the posterior CC and was not seen in the genu or the body. During development, the rudimentary CC originates in the anterior body at 11–13 wk GA, then the CC expands in both anterior and posterior directions and forms the genu and posterior body, followed finally by the splenium (31,32). After formation of the basic CC by ~20 wk GA (33), the genu exhibits rapid growth which then slows after birth (32), whereas growth of the splenium accelerates after birth. Thus, the posterior CC, especially the splenium, develops most slowly among the CC subdivisions, which may account for the predominance of FA changes in the posterior CC in our study. It is also possible that the maturational state of oligodendrocytes (OLs) play a role in selective injury to the

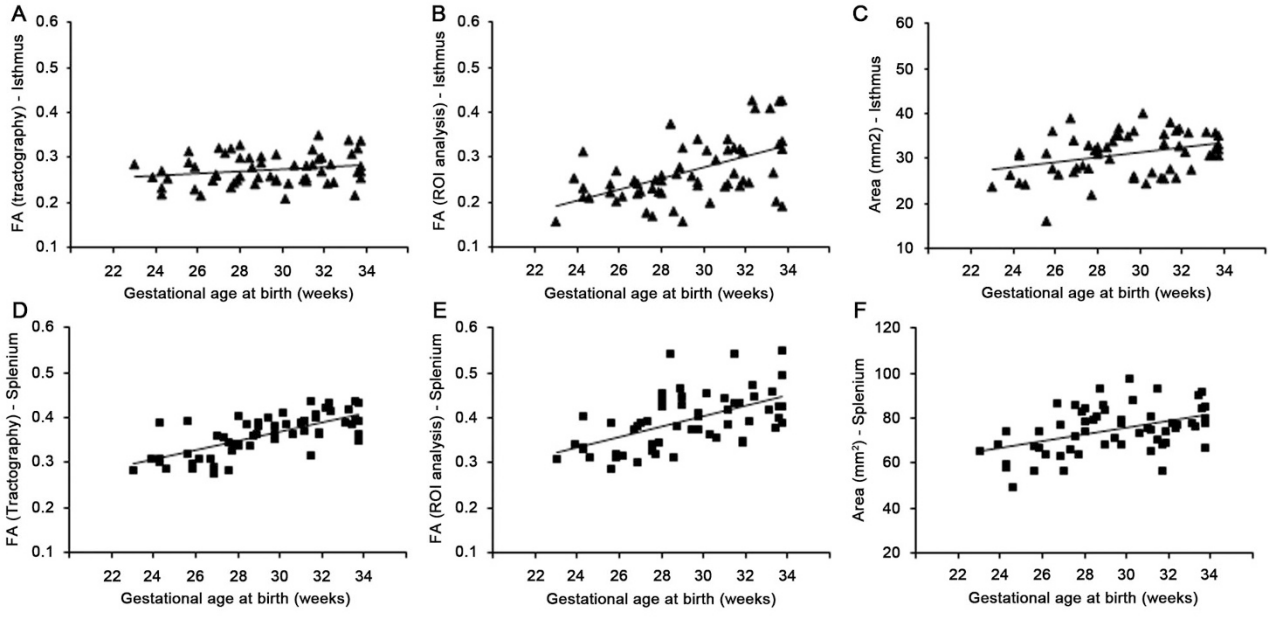

Figure 4. Relationship between FA or size of posterior CC and GA at birth. Graphs demonstrate FA measured by tractography (*A* and *D*), FA measured by manual ROI analysis (*B* and *E*), and cross-sectional area (*C* and *F*) in relation to GA at birth. There were significant correlations between GA at birth and FA measured by tractography of the splenium [(*D*) $p < 0.001$, $r = 0.70$], FA measured by ROI analysis of isthmus [(B) $p < 0.001$, $r = 0.51$] and splenium [(E) $p < 0.001$, $r = 0.59$], and area of the isthmus [(*C*) $p = 0.013$, $r = 0.33$] and splenium [(*F*) $p = 0.002$, $r = 0.42$]. (*A*) There was no correlation between FA measured by tractography of the isthmus and GA at birth ($p = 0.16$, $r = 0.18$).

posterior CC. OLs develop from progenitor OLs to pre-OLs, immature OLs, and finally to mature OLs (33), and there is evidence to suggest that pre-OLs are particularly vulnerable to injury (34). Because the posterior CC develops later than the rest of the CC, the OL lineage during the early fetal stage is more immature and constitutes predominantly pre-OLs (35). When these pre-OLs receive the stress attributed to premature birth, they can be directly injured and become arrested in the pre-OL phenotype, unable to mature (36). The differentiation of pre-OLs into immature OLs has also been shown to coincide with increasing FA in the rodent brain (37,38). Thus, in our study, the reduced FA in the posterior CC in term infants born at the younger GA may relate to impaired OL maturation. However, we could not determine whether the FA decline and size reduction in the posterior CC were related to WM injury or maturational delay.

There were no differences in ADC values in the various CC subdivisions among the different GA groups in our study. Previous reports suggest the ADC can be altered by WM maturation and/or injury as detected by conventional MRI (18,39). Because we used subjects with no detectable WM changes on conventional MR, this may account for the lack of ADC changes. These data also suggest that the FA is more sensitive than ADC for assessing WM injury.

We observed significant reductions in the sizes of the isthmus and the splenium in the youngest GA infants (group A) at term-equivalent age, and there was a significant correlation with GA at birth. These results are supported by previous studies examining CC size in children and adolescents born preterm (9–12). Furthermore, the thinning of the posterior CC observed in our study matched the pattern of FA decline of the posterior CC. Finally, as the FA measured by DTI, particularly by ROI analysis, tended to exhibit a stronger correlation with GA at birth compared with cross-sectional area, DTI may be a more sensitive measure of assessing CC injury than manual area measurement.

As discussed herein, we demonstrated characteristics of the CC in preterm infants without apparent WM lesions at term-equivalent age using both tractography and ROI analysis. ROI analysis is a simple method to perform but is operator dependent and has lower reproducibility (16). By contrast, tractography is slightly more objective because the ROIs for tract depiction can be placed to cover a relatively large area, improving reproducibility (13). Irrespective of the DTI method selected, DTI remains inherently limited by the presence of crossing fibers in target WM tracts (40,41), which may account for our inability to detect a significant difference in the isthmus using tractography. When ROI analysis is used for the midsagittal slice of the CC, the measured FA is less affected by crossing fibers as the majority of midsagittal CC fibers are aligned in a single direction. Thus, development of the CC, particularly at the isthmus, may be more reliably assessed using ROI analysis.

A limitation of this study is that we could not compare data of late preterm (34–36 wk GA) and normal term born infants because of the insufficient numbers of normal subjects. As it is not our clinical routine to perform MRI on infants without risk of brain damage, MR was performed on infants born at <34 wk GA who had risk of PVL. Of note, even in the absence of comparison with late preterm and normal term infants, there was clear correlation between the severity of FA decline in the posterior CC and the degree of the prematurity.

Further studies are required to assess neurodevelopmental outcomes of our subjects, particularly cognitive function that is associated with development of the posterior CC (6–8,10–12). By showing an association between DTI parameters and neurodevelopmental outcome, quantitative DTI assessment at term-equivalent age may be useful for screening preterm born infants for prediction of future neurodevelopmental impairments.

REFERENCES

1. Platt MJ, Cans C, Johnson A, Surman G, Topp M, Torrioli MG, Krageloh-Mann I 2007 Trend in cerebral palsy among infants of very low birthweight (<1500 g) or born prematurely (<32 weeks) in 16 European centres: a database study. Lancet 369:43–50
2. Saigal S, Doyle LW 2008 An overview of mortality and sequelae of preterm birth from infancy to adulthood. Lancet 371:261–269
3. Marlow N, Wolke D, Bracewell MA, Samara M; EPICure Study Group 2005 Neurologic and developmental disability at six of age after extremely preterm birth. N Engl J Med 352:9–19
4. Anderson PJ, Doyle LW 2008 Cognitive and educational deficits in children born extremely preterm. Semin Perinatol 32:51–58
5. Woodward LJ, Anderson PJ, Austin NC, Howard K, Inder TE 2006 Neonatal MRI to predict neurodevelopmental outcomes in preterm infants. N Engl J Med 355:685–694
6. Stewart AL, Rifkin L, Amess PN, Kirkbride V, Townsend JP, Miller DH, Lewis SW, Kingsley DP, Moseley IF, Foster O, Murray RM 1999 Brain structure and neurocognitive and behavioural function in adolescents who were born very preterm. Lancet 353:1653–1657
7. Kontis D, Catani M, Cuddy M, Walshe M, Nosarti C, Jones D, Wyatt J, Rifkin L, Murray R, Allin M 2009 Diffusion tensor MRI of the corpus callosum and cognitive function in adults born preterm. Neuroreport 20:424–428
8. Fryer SL, Frank LR, Spadoni AD, Theilmann RJ, Nagel BJ, Schweinsburg AD, Tapert SF 2008 Microstructural integrity of the corpus callosum linked with neuropsychological performance in adolescents. Brain Cogn 67:225–233
9. Peterson BS, Vohr B, Staib LH, Cannistraci CJ, Dolberg A, Schneider KC, Katz KH, Westerveld M, Sparrow S, Anderson AW, Duncan CC, Makuch RW, Gore JC, Ment LR 2000 Regional brain volume abnormalities and long-term cognitive outcome in preterm infants. JAMA 284:1939–1947
10. Nagy Z, Westerberg H, Skare S, Andersson JL, Lilja A, Flodmark O, Fernell E, Holmberg K, Bohm B, Forssberg H, Lagercrantz H, Klingberg T 2003 Preterm children have disturbances of white matter at 11 years of age as shown by diffusion tensor imaging. Pediatr Res 54:672–679
11. Nosarti C, Rushe TM, Woodruff PW, Stewart AL, Rifkin L, Murray RM 2004 Corpus callosum size and very preterm birth: relationship to neuropsychological outcome. Brain 127:2080–2089
12. Narberhaus A, Segarra D, Caldu X, Gimenez M, Junque C, Pueyo R, Botet F 2007 Gestational age at preterm birth in relation to corpus callosum and general cognitive outcome in adolescents. J Child Neurol 22:761–765
13. Mori S, van Zijl PC 2002 Fiber tracking: principles and strategies—a technical review. NMR Biomed 15:468–480
14. Beaulieu C 2002 The basis of anisotropic water diffusion in the nervous system—a technical review. NMR Biomed 15:435–455
15. Neil J, Miller J, Mukherjee P, Huppi PS 2002 Diffusion tensor imaging of normal and injured developing human brain—a technical review. NMR Biomed 15:543–552
16. Dubois J, Hertz-Pannier L, Dehaene-Lambertz G, Cointepas Y, Le Bihan D 2006 Assessment of the early organization and maturation of infants' cerebral white matter fiber bundles: a feasibility study using quantitative diffusion tensor imaging and tractography. Neuroimage 30:1121–1132
17. Gilmore JH, Lin W, Corouge I, Vetsa YS, Smith JK, Kang C, Gu H, Hamer RM, Lieberman JA, Gerig G 2007 Early postnatal development of corpus callosum and corticospinal white matter assessed with quantitative tractography. AJNR Am J Neuroradiol 28:1789–1795
18. Provenzale JM, Liang L, DeLong D, White LE 2007 Diffusion tensor imaging assessment of brain white matter maturation during the first postnatal year. AJR Am J Roentgenol 189:476–486
19. Gao W, Lin W, Chen Y, Gerig G, Smith JK, Jewells V, Gilmore JH 2009 Temporal and spatial development of axonal maturation and myelination of white matter in the developing brain. AJNR Am J Neuroradiol 30:290–296
20. Arzoumanian Y, Mirmiran M, Barnes PD, Woolley K, Ariagno RL, Moseley ME, Fleisher BE, Atlas SW 2003 Diffusion tensor brain imaging findings at term-equivalent age may predict neurologic abnormalities in low birth weight preterm infants. AJNR Am J Neuroradiol 24:1646–1653
21. Counsell SJ, Shen Y, Boardman JP, Larkman DJ, Kapellou O, Ward P, Allsop JM, Cowan FM, Hajnal JV, Edwards AD, Rutherford MA 2006 Axial and radial

diffusivity in preterm infants who have diffuse white matter changes on magnetic resonance imaging at term-equivalent age. Pediatrics 117:376–386
22. Anjari M, Srinivasan L, Allsop JM, Hajnal JV, Rutherford MA, Edwards AD, Counsell SJ 2007 Diffusion tensor imaging with tract-based spatial statistics reveals local white matter abnormalities in preterm infants. Neuroimage 35:1021–1027
23. Rose SE, Hatzigeorgiou X, Strudwick MW, Durbridge G, Davies PS, Colditz PB 2008 Altered white matter diffusion anisotropy in normal and preterm infants at term-equivalent age. Magn Reson Med 60:761–767
24. Huang H, Zhang J, Jiang H, Wakana S, Poetscher L, Miller MI, van Zijl PC, Hillis AE, Wytik R, Mori S 2005 DTI tractography based parcellation of white matter: Application to the mid-sagittal morphology of corpus callosum. Neuroimage 26:195–205
25. Catani M, Jones DK, Donato R, Ffytche DH 2003 Occipito-temporal connections in the human brain. Brain 126:2093–2107
26. Witelson SF 1989 Hand and sex differences in the isthmus and genu of the human corpus callosum. Brain 112:799–835
27. Hofer S, Frahm J 2006 Topography of the human corpus callosum revisited—comprehensive fiber tractography using diffusion tensor magnetic resonance imaging. Neuroimage 32:989–994
28. Park HJ, Kim JJ, Lee SK, Seok JH, Chun J, Kim DI, Lee JD 2008 Corpus callosum connection mapping using cortical gray matter parcellation and DT-MRI. Hum Brain Mapp 29:503–516
29. Davatzikos C, Barzi A, Lawrie T, Hoon AH Jr, Melhem ER 2003 Correlation of corpus callosal morphometry with cognitive and motor function in periventricular leukomalacia. Neuropediatrics 34:247–252
30. Fan GG, Yu B, Quan SM, Sun BH, Guo QY 2006 Potential of diffusion tensor MRI in the assessment of periventricular leukomalacia. Clin Radiol 61:358–364
31. Rakic P, Yakovlev PI 1968 Development of the corpus callosum and cavum septi in man. J Comp Neurol 132:45–72
32. Kier EL, Truwit CL 1996 The normal and abnormal genu of the corpus callosum: an evolutionary, embryologic, anatomic, and MR analysis. AJNR Am J Neuroradiol 17:1631–1641
33. Volpe JJ 2008 Neurology of the Newborn. 5th ed. Saunders, Philadelphia, pp 96–98
34. Back SA, Riddle A, McClure MM 2007 Maturation-development vulnerability of perinatal white matter in premature birth. Stroke 38:724–730
35. Back SA, Luo NL, Borenstein NS, Levine JM, Volpe JJ, Kinney HC 2001 Late oligodendrocyte progenitors coincide with the developmental window of vulnerability for human perinatal white matter injury. J Neurosci 21:1302–1312
36. Segovia KN, McClure M, Moravec M, Luo NL, Wan Y, Gong X, Riddle A, Craig A, Struve J, Sherman LS, Back SA 2008 Arrested oligodendrocyte lineage maturation in chronic perinatal white matter injury. Ann Neurol 63:520–530
37. Prayer D, Barkovich AJ, Kirschner DA, Prayer LM, Roberts TP, Kucharczyk J, Mosely ME 2001 Visualization of nonstructural change in early white matter development on diffusion-weighted MR images: evidence supporting premyelination anisotropy. AJNR Am J Neuroradiol 22:1572–1576
38. Drobyshevsky A, Song SK, Gamkrelidze G, Wyrwicz AM, Derrick M, Meng F, Li L, Ji X, Trommer B, Beardsley DJ, Luo NL, Back SA, Tan S 2005 Developmental changes in diffusion anisotropy coincide with immature oligodendrocyte progression and maturation of compound action potential. J Neurosci 25:5988–5997
39. Miller SP, Vigneron DB, Henry RG, Bohland MA, Ceppi-Cozzio C, Hoffman C, Newton N, Partridge JC, Ferriero DM, Barkovich AJ 2002 Serial quantitative diffusion tensor MRI of the premature brain: development in newborns with and without injury. J Magn Reson Imaging 16:621–632
40. Wiegell MR, Larsson HB, Wedeen VJ 2000 Fiber crossing in human brain depicted with diffusion tensor MR imaging. Radiology 217:897–903
41. Oouchi H, Yamada K, Sakai K, Kizu O, Kubota T, Ito H, Nishimura T 2007 Diffusion anisotropy measurement of brain white matter is affected by voxel size: underestimation occurs in area with crossing fiber. AJNR Am J Neuroradiol 28:1102–1106